Vol 14 No 8, August 2005
1009-1963/2005/14(08)/1585-06

Chinese Physics

© 2005 Chin. Phys. Soc.
and IOP Publishing Ltd

# The validity of high-pass angular spectrum filter in solid immersion lens system

Zheng Chong-Wei(郑崇伟)[a)†] and Dai Yu-Xing(戴瑜兴)[b)]

[a)] *Department of Physics & Electronic Information Scinece , Wenzhou University, Wenzhou 325027, China*

[b)] *College of Electrical and Information Engineering, Hunan University, Changsha 410082, China*

(Received 18 November 2004; revised manuscript received 27 April 2005)

The focal field of a solid immersion lens (SIL) system with a high-pass angular spectrum filter is calculated by using a vector method. Numerical results show that for a radially (azimuthally) polarized input field, a high-pass angular spectrum filter can reduce the light-spot (dark-spot) size of the SIL system. For a linearly polarized input field, however, the focal field cannot be optimized and the optical storage density of the SIL system cannot be improved by using a simple high-pass filter, either.

**Keywords:** solid immersion lens, polarization, high-pass filter
**PACC:** 4280B, 4230H, 4225F,4230N

## 1. Introduction

Relieving the limits imposed by diffraction in imaging systems has long been a much interesting subject because of its potential applications in a number of important fields. There exist a variety of approaches to improve the resolution of an optical system, such as designing high numerical-aperture (NA) lenses,[1] the method of a solid immersion lens (SIL)[2] and oil immersion lens,[3] the scanning near-field optical microscopy,[4] the multilevel optical data recording on phase-change media,[5] the three-dimensional storage by parallel writing in poly-methyl methacrylate (PMMA) with femtosecond laser pulses,[6] and using the diffractive supperresolution elements.[7] High-pass amplitude or phase filters have been applied to optimize the focal field distribution for low-NA systems.[7−11] For a high-NA SIL system, Lu and co-authors obtained a conclusion that a two-zone amplitude[12] and phase[13] filter could increase the storage density of the SIL system. Recently, Zhang *et al*[14] pointed out that a simple two-zone phase filter could not decrease the focal spot size of the high-NA SIL. To improve the resolution of an SIL, a three-zone phase or more phase-zone filter is desired.[15] In this paper, we apply the formula presented by Helseth[15] to calculate the optical distribution of the SIL system with a high-pass amplitude filter and find whether a two-zone amplitude filter can improve the resolution of high-NA SIL systems depends on the polarization of input field.

## 2. Linearly polarized input field

The calculated model is schemed as shown in Fig.1. A hemispherical SIL is placed behind a converging lens with a focus on the plane facet of SIL. The existence of SIL increases the effective numeric aperture of an objective, which results in a smaller optical spot. A two-zone annular filter is closely placed in front of the converging lens. The shaded part at the centre of the objective lens is called a high-pass angular spectrum filter, and it is used to shelter the light, which will form a low spatial frequency part in the convergent laser behind the objective lens. Of course, this filter will lose the laser intensity, which is not unfavourable to the optical storage.

The incident laser is assumed to be polarized along the $x$-axis. The numeric aperture of the objective lens is equal to $\sin\alpha$ (where $\alpha$ is the convergence angle). The optical distributions in this paper are drawn in a plane 100 nm away from the plane facet of SIL without special indication.

†E-mail: zcw@wznc.zj.cn

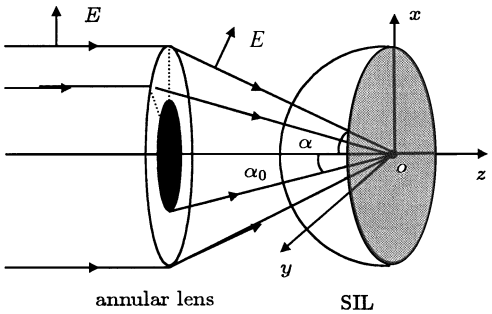



**Fig.1.** The scheme of an annular solid immersion system. $\alpha$ is the convergence angle of lens and $\alpha_0$ is the obstructed convergence angle.

According to the formulae given in Ref.[15], the transmitted field of the SIL with a high-pass filter can be expressed as

$$\begin{aligned} E_x(r,\varphi,z) &= -\mathrm{i}\left[I_0(r,z) + I_2(r,z)\cos 2\varphi\right], \\ E_y(r,\varphi,z) &= -\mathrm{i}I_2(r,z)\sin 2\varphi, \\ E_z(r,\varphi,z) &= -2I_1(r,z)\cos\varphi, \end{aligned} \tag{1}$$

where $I_{0,1,2}$ are integrals over the aperture angle $\theta$ in the emergent pupil plane as seen from the focus, and $\varphi$ represents the angle included between the polarization direction of the incident field and the observation meridian plane. $I_{0,1,2}$ can be given by

$$\begin{aligned} I_0 &= \int_{\alpha_0}^{\alpha} \sqrt{\cos\theta}\sin\theta\left(t_s + t_p\sqrt{1-\left(\frac{n_1}{n_2}\sin\theta\right)^2}\right) J_0(kn_1 r\sin\theta)\exp\left[\mathrm{i}kn_2 z\sqrt{1-\left(\frac{n_1}{n_2}\sin\theta\right)^2}\right]\mathrm{d}\theta, \\ I_1 &= \int_{\alpha_0}^{\alpha} \sqrt{\cos\theta}\sin\theta\, t_p\sqrt{1-\left(\frac{n_1}{n_2}\sin\theta\right)^2} J_1(kn_1 r\sin\theta)\exp\left[\mathrm{i}kn_2 z\sqrt{1-\left(\frac{n_1}{n_2}\sin\theta\right)^2}\right]\mathrm{d}\theta, \\ I_2 &= \int_{\alpha_0}^{\alpha} \sqrt{\cos\theta}\sin\theta\left[t_s - t_p\sqrt{1-\left(\frac{n_1}{n_2}\sin\theta\right)^2}\right] J_2(kn_1 r\sin\theta)\exp\left[\mathrm{i}kn_2 z\sqrt{1-\left(\frac{n_1}{n_2}\sin\theta\right)^2}\right]\mathrm{d}\theta, \end{aligned} \tag{2}$$

where $\alpha_0$ is the obstructed convergence angle, $t_s$ and $t_p$ are the Fresnel coefficients through the planar dielectric interface, $J_m$ is the $m$th-order Bessel function of the first kind, $k = 2\pi/\lambda$, and $\lambda$ is the illumination wavelength, $\sqrt{\cos\theta}$ is a sine apodization function, $n_1$ and $n_2$ are, respectively, the refractive indices of the SIL and the dielectric medium in the image space.

We give some numerical simulations in the following. In all simulations of this paper, we use the same parameters as those in Ref.[12]. The wavelength is set as 532nm. The maximum incident angle is 60° i.e. the NA of the objective lens is 0.86. The refractive index of the SIL is set as $n_1$=2, and the refractive index of the image medium is $n_2$=1, i.e. the total internal reflect critical angle is 30°.

For the $x$-polarized plane-wave input field, Figs.2(a) and (b) show the light intensity distributions of the field components and the contour of total field just before and after the light passes through the plane facet of SIL, respectively. The intensity distribution no longer has rotational symmetry, although the input-field intensity is rotationally symmetric. The intensity ratio $I_x$:$I_y$:$I_z$ of the three polarization components varies from $1 : 0.34\times10^{-3} : 0.13$ (Fig.2(a)) to $1 : 0.03 : 0.48$ (Fig.2(b)). Clearly, the $y$ and $z$components are increased greatly. The $z$component has an important effect on the shape of spot. The isointensity contour lines resemble the shape of ellipse before the light passes through the plane facet of SIL (see Fig.2(a) (IV)). However, after the light passes through the plane facet of SIL, the shape of the spot more or less is of an ellipse but largely enlarged along the $x$-direction (Fig.2(b) (IV)). Figures 3(a) and (b) show a comparison between the field distributions along the $x$ direction and the $y$ direction respectively. The FWHM (the full-width at half-maximum) at the $y$-axis is almost unchanged (only increases by 2%), but the FWHM at the $x$-axis increases by 49% after the light passes through the plane facet. The FWHM of spot at the $x$-axis has a remarkable change resulting from the stronger $z$-component which is distributed in the vicinity of the $x$-axis.

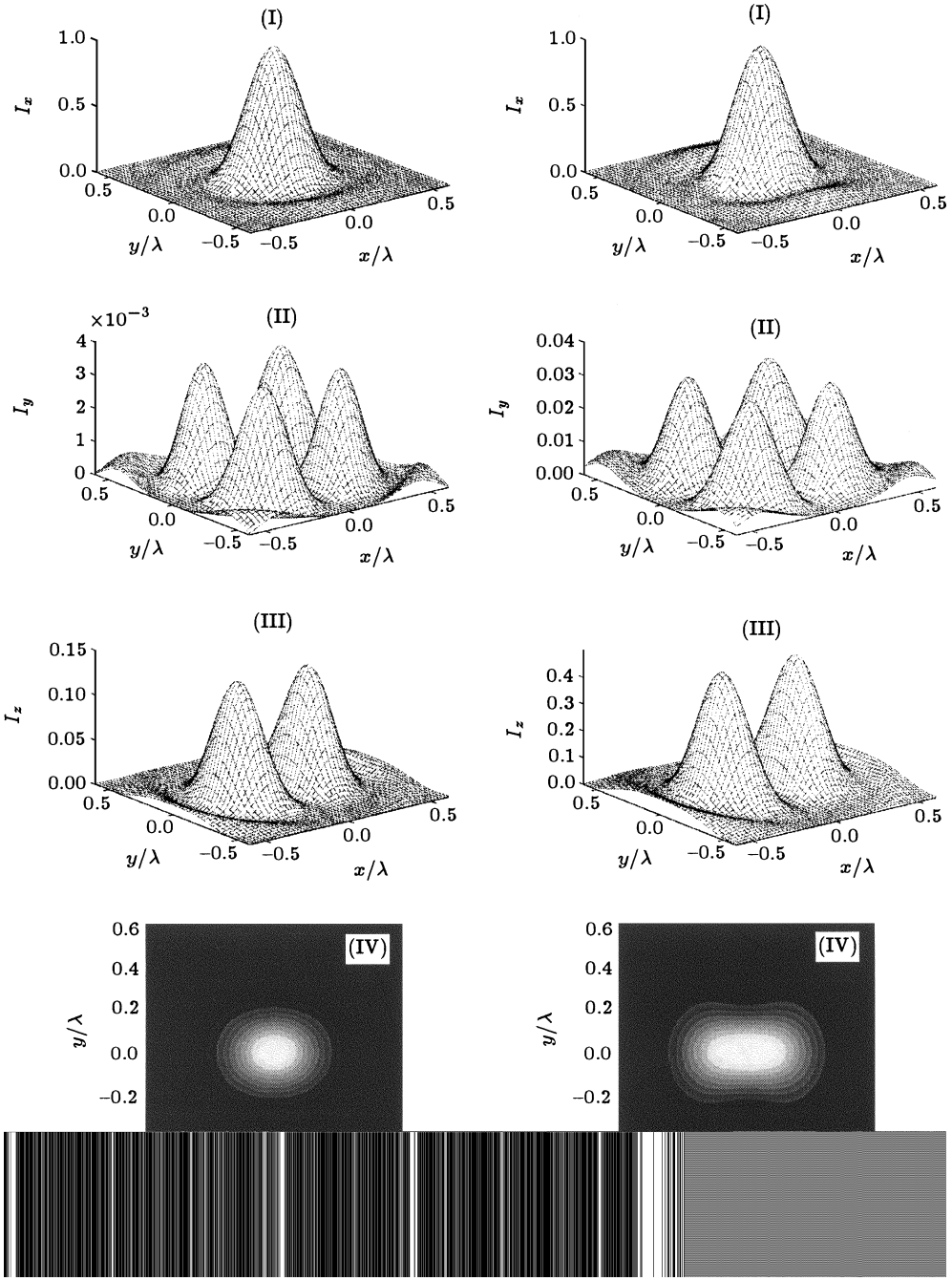



**Fig.2.** Intensity distributions before (a) and after (b) the light passes through the plane facet of SIL when the incident light is the $x$-polarized light. (I) The $x$-polarized component. (II) The $y$-polarized component. (III) The $z$-polarized component. (IV) The contour for total intensity.

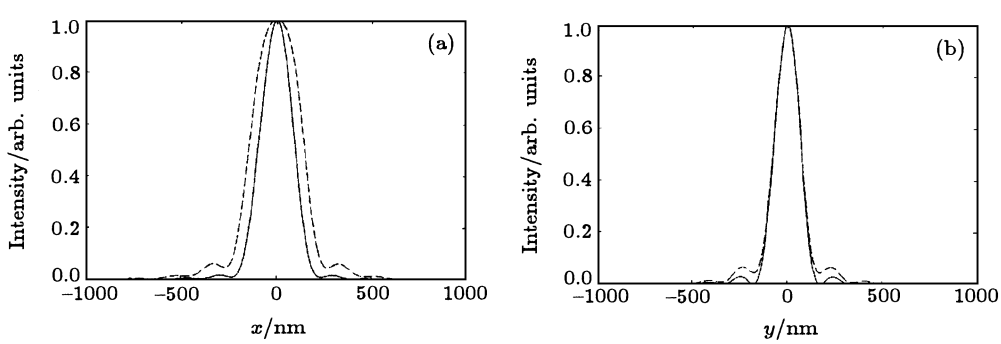



**Fig.3.** The light intensity distribution for (a) along $x$-axis and (b) along $y$-axis. Solid line is drawn before the light transmits through the facet of SIL; the dashed one is drawn behind the facet. The incident light is the $x$-polarized light.

From the scalar theory of diffraction it is well known that introducing a high-pass filter reduces the spot size.[7,8] However, the side lobes become more pronounced, which leads to a reduced peak intensity. In the next step we examine whether using an annular high-pass filter can reduce the spot sizes in vector theory of diffraction. Figure 4 shows the contour of the intensity at $z$=100 nm apart from the SIL. A comparison between the optical distribution contours in two cases is shown in Fig.4. It is seen from Fig.4 that the isointensity contour lines resemble more or less the shape of ellipses without filters. However, the shape of the spot is strongly deformed and has the shape of a bone rather than the shape of an ellipse when the annular high-pass filter of $\theta_{\rm f} = 30^\circ$ is placed in front of the lens. And the side lobes are very pronounced, reaching values of ranging from about 15% to 23% of the maximum intensity of spot, which depends on the direction of observation (see Fig.5). Surprisingly, the FWHM at the $x$-axis increases by 23% (see Fig.5(a)) rather than decreasing by 40%.[12] The FWHM at the $y$-axis decreases by 29%, which is close to 33% in Ref.[12] because the strong $z$-component is distributed in the vicinity of the $x$-axis and it does not make any contribution to the intensity at the $y$-axis. After the insertion of the high-pass filter the intensity of the $z$-component increases from 47% to 80% relative to the intensity of the $x$-component.

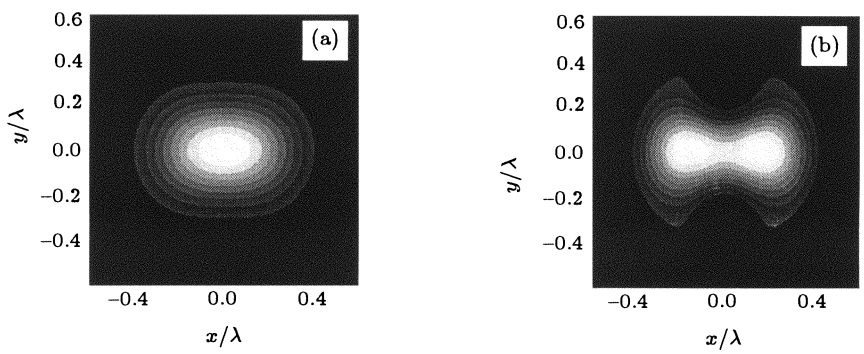



**Fig.4.** Comparison between the contours of the field distributions in a plane 100 nm apart from the plane facet of SIL: (a) without filters, (b) with an annular high-pass filter at an obscuration angle of $\theta_{\rm f} = 30^\circ$. The incident light is the $x$-polarized light.

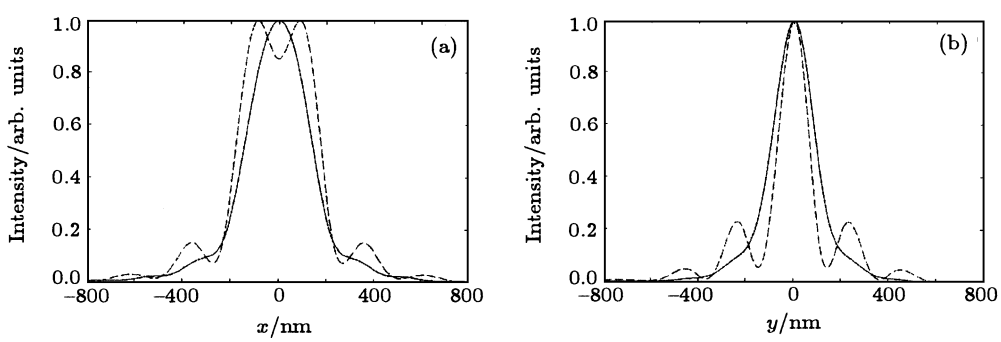



**Fig.5.** Light intensity distribution in a plane 100 nm apart from the plane facet of SIL when the incident light is the $x$-polarized light: (a) along the $x$-axis and (b) along the $y$-axis. Solid curve is for the case without filters and the dashed curve is for the case with a filter of $\theta_{\rm f} = 30^\circ$.

## 3. Radially polarized input field

To simplify the calculations and examine the effects of a filter, we assume a radially polarized input field in cylindrical coordinates to be

$$\boldsymbol{E}_0(r,\varphi,z) = \boldsymbol{e}_r. \tag{3}$$

This input illuminates the SIL with a high-pass filter and we can obtain the transmitted fields as follows:

$$\begin{aligned} E_r(r,\varphi,z) &= \int_{\alpha_0}^{\alpha} \sqrt{\cos\theta}\sin\theta\, I_r \mathrm{d}\theta, \\ E_\varphi(r,\varphi,z) &= 0, \\ E_z(r,\varphi,z) &= \int_{\alpha_0}^{\alpha} \sqrt{\cos\theta}\sin\theta\, I_z \mathrm{d}\theta, \end{aligned} \tag{4}$$

where

$$I_r = \mathrm{i}\sqrt{1-\left(\frac{n_1}{n_2}\sin\theta\right)^2}\, t_p J_1(krn_1\sin\theta) \times \exp\left[\mathrm{i}kn_2 z\sqrt{1-\left(\frac{n_1}{n_2}\sin\theta\right)^2}\right],$$

$$I_z = \frac{n_1}{n_2}\sin\theta\, t_p J_0(krn_1\sin\theta) \times \exp\left[\mathrm{i}kn_2 z\sqrt{1-\left(\frac{n_1}{n_2}\sin\theta\right)^2}\right]. \quad (5)$$

In contrast to the case for linearly polarized input field, the high-pass filter can reduce the spot size of the radially polarized input field, as shown in Fig.6. The FWHM of spot decreases by 27%, i.e. from 224nm without filters to 163nm with a filter of $\theta_{\mathrm{f}} = 30°$. Both the radial and the longitudinal field intensities are rotationally symmetric. The high-pass filter reduces the size of the longitudinal field, which is different from the case for linearly polarized input field in Section 3. Moreover, the side lobes of the total intensity distribution are less pronounced, i.e. the peak values of the side lobes's intensity are less than 11% of the intensity at the centre (Fig.6(b)).

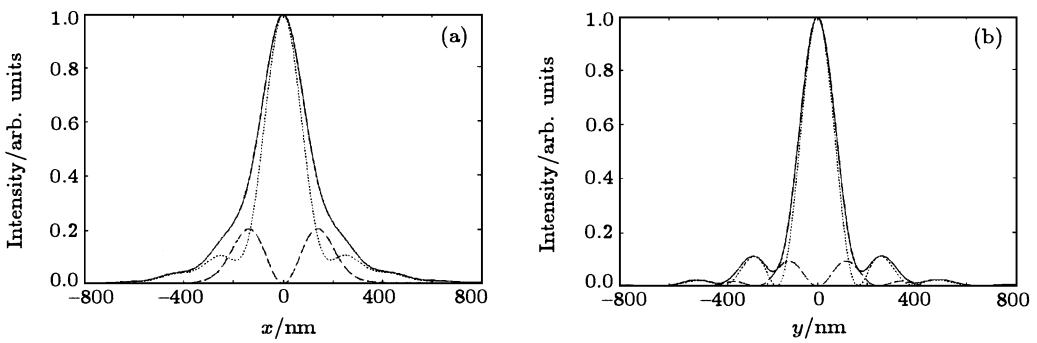



**Fig.6.** Light intensity distribution in a plane 100nm apart from the plane facet of SIL for radially polarized input field. (a) without filters and (b) with a filter of $\theta_{\mathrm{f}} = 30°$. The solid curve denotes the total intensity distribution, the dashed curve is for the transverse component of the field, and the dotted curve is for the axial component.

## 4. Azimuthally polarized input field

In a way similar to that in the case of radially polarized input field, we assume that the SIL is illuminated by an azimuthally polarized input field

$$\boldsymbol{E}_0(r,\varphi,z) = \boldsymbol{e}_\varphi. \quad (6)$$

The transmitted fields of the SIL can be written as

$$E_r(r,\varphi,z) = 0,$$
$$E_\varphi(r,\varphi,z) = \int_{\alpha_0}^{\alpha}\sqrt{\cos\theta}\sin\theta\, I_\varphi \mathrm{d}\theta,$$
$$E_z(r,\varphi,z) = 0, \quad (7)$$

where

$$I_\varphi = t_s J_1(krn_1\sin\theta) \times \exp\left[\mathrm{i}kn_2 z\sqrt{1-\left(\frac{n_1}{n_2}\sin\theta\right)^2}\right]. \quad (8)$$

In this case we find that only one vector component in the azimuthal direction of the field is rotationally symmetric. The azimuthally polarized beam in the field is similar to the radial component of the radially polarized beam, except the phase of the electric field being rotated by 90°. Surprisingly, after the light passes through an SIL, the uniform intensity distribution of the input field becomes a doughnut-shape intensity distribution. This doughnut-mode field has extensive applications in the guiding and trapping of atom.[16,17] The high-pass filter reduces the dark-hollow beam size of this doughnut field, as shown in Fig.7.

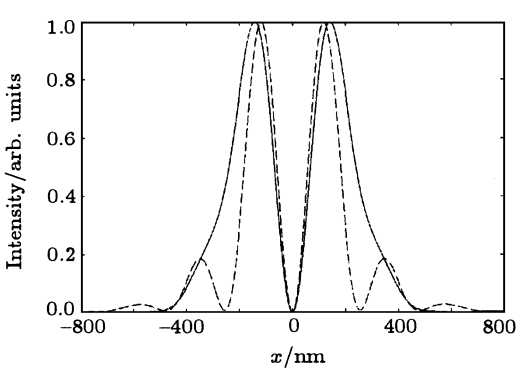



**Fig.7.** Light intensity distribution in a plane 100nm apart from the plane facet of SIL for azimuthally polarized input field. Solid curve is for the case without filters and the dashed curve is for the case with a filter of $\theta_{\mathrm{f}} = 30°$.

## 5. Conclusion

In conclusion, we have presented a detailed comparison for three different input fields passing through a high-NA SIL system. We find that a two-zone high-pass filter cannot improve the optical storage density of an SIL system when the input field is a linearly polarized beam. This conclusion is contrary to that in Ref.[12]. The error in Ref.[12] is caused mainly by neglecting the $x$- and $y$-polarized components, and partly by using the far-field approximation to the lens. The numerical calculation and analysis in Section 2 have shown that the $z$-component is very strong and it is not neglected. However, when the input field is radially polarized, a two-zone high-pass filter can reduce the spot size and improve the optical storage density of an SIL system. For the azimuthally polarized input field with a uniform intensity distribution, a high-pass filter can reduce the central dark-spot size and it is useful to the guiding and trapping of atom.

## References


[1] Sheppard C J R and Matthews H J 1987 *J. Opt. Soc. Am.* A **4** 1354

[2] Mansfield S M and G S Kino 1990 *Appl. Phys. Lett.* **57** 2615

[3] Martini N, Bewersdory J and Hell S W 2002 *J. Microsc.* **206** 146

[4] Török P, Sheppard C J R and Varga P 1996 *J. Mod. Opt.* **43** 1167

[5] Xiao J X, Qi G S, She P and Xu D Y 2003 *Chin. Phys.* **12** 1241

[6] Cheng G H, Wang Y S, Liu Q, Zhao W and Chen G F 2004 *Acta Phys. Sin.* **52** 436 (in Chinese)

[7] Sales T R M and Morris G M 1997 *J Opt. Soc. Am.* A **14** 1637

[8] Zhang Y 2003 *Optik* **114** 76

[9] Jia J, Zhou C and Liu L 2003 *Opt. Commun.* **228** 271

[10] Sales T R M and Morris G M 1998 *Opt. Commun.* **156** 227

[11] Sheppard C J R 1997 *Optik* **48** 329

[12] Lu Y, Xie J, Zhang J, Ming H and Wang P 2002 *Opt. Commun.* **203** 87

[13] Lu Y, Xie J and Ming H 2003 *Opt. Commun.* **215** 251

[14] Zhang Y, Xiao H and Zheng C 2004 *New J. Phys.* **6** 75

[15] Helseth L E 2001 *Opt. Commun.* **191** 161

[16] Arlt J, Hitomi T and Dholakia K 2000 *Appl. Phys.* B **71** 549

[17] Rhodes D P, Lancaster G P T, Livesey J, McGloin D, Arlt J and Dholakia K 2002 *Opt. Commun.* **214** 247